

Some classification of fragmentation processes related to fracture

This article has been downloaded from IOPscience. Please scroll down to see the full text article.

2000 J. Phys. A: Math. Gen. 33 2179

(<http://iopscience.iop.org/0305-4470/33/11/301>)

View [the table of contents for this issue](#), or go to the [journal homepage](#) for more

Download details:

IP Address: 171.66.16.118

The article was downloaded on 02/06/2010 at 08:02

Please note that [terms and conditions apply](#).

Some classification of fragmentation processes related to fracture

A Bershadskii

Machanaim Center, PO Box 39953, Ramat-Aviv 61398, Tel-Aviv, Israel

and

Department of Physics, The Chinese University of Hong Kong, Shatin, N.T., Hong Kong

Received 27 September 1999, in final form 17 January 2000

Abstract. Nonlinear parametric Kubo noise is suggested to approximate the effective rate of crack branch growth. It is shown that the parameter of nonlinearity of this parametric noise can be used to classify the size probability distributions observed in numerous experiments and numerical simulations on fragmentation processes related to fracture.

1. Introduction

A recent experiment [1] with fast straight crack instability in a brittle polymer (PMMA) shows that the instability leads to the appearance of numerous left- and right-side micro-branches which live a short time and then die. The authors of [1] observed a log-normal distribution of the micro-branch lengths. Fragmentation processes related to fracture are often characterized by log-normal distribution as well. Therefore, the authors of [1] (see also [2]) assume that the probability distribution of the fragment sizes is directly related to the corresponding distribution of the crack branch lengths. In this paper we use this rather plausible hypothesis to classify possible types of probability distributions of the fragment sizes in fragmentation processes related to fracture. It should be noted that the power-law distributions of fragment sizes are also widely observed in numerical simulations and experiments [3–8]. Although the exponents of these distributions depend on the conditions (on the space dimension, in particular) some ‘attractive’ values of the exponent can be noted. Deviations from these ‘attractive’ values could be related to anisotropy and to some type of intermittency (see below). Therefore, a classification of the probability distributions observed in the experiments and numerical simulations seems to be useful at this stage.

2. Model

If we consider a statistical assembly of branches, then the length $l(t)$, which a given branch may choose from a broad distribution, is a random function of the time of the process, t . Moreover, the mean (on the assembly) value $\langle l(t) \rangle$ can be a decreasing function of time due to the branches’ creation and death processes. Let us consider an effective Langevin equation describing the propagation of the tip of a crack branch

$$m_e \frac{d^2 l}{dt^2} = F - F_f$$

where m_e is some constant (the effective mass of the tip), F is the force term depending on l and t , and F_f is a dissipative term depending on dl/dt . Different expressions are suggested for the dissipative term. The simplest expression, $F_f = c dl/dt$, is related to the effective friction (see, for instance, [9–11]). For large friction constants c we may neglect the second derivative with respect to time (the inertial term) and obtain the approximation

$$c \frac{dl}{dt} = F(l, t).$$

A short correlated fluctuating force $F(l, t)$ may be represented as a space-modulated white noise

$$F(l, t) = A(l)\eta(t)$$

where $\eta(t)$ is white noise. If the large-scale cutoff $L \gg l_m$ (where l_m is microscale of the branches), then one can expect that in the interval $L \gg l \gg l_m$ the scale invariance takes place and, consequently, the amplitude scales as $A(l) \sim l^n$. Then, finally, in the scaling interval,

$$\frac{dl}{dt} \simeq \eta(t)l^n \quad (1)$$

where

$$\langle \eta(t)\eta(t') \rangle = 2\sigma^2 \delta(t - t') \quad (2)$$

and σ is some constant. Thus, the effective rate of the branch length growth is represented as nonlinear parametric Kubo noise. Different values of the parameter of nonlinearity ($n = 1, 2, 3$) characterize different topology of the manifolds (point-like, front-like, and volume-like) where the nucleation of a crack preferably occurs.

For $n = 1$, using substitution $y = \ln l$, (in the Stratonovich approach), equation (1) can be transformed into the simplest diffusion equation

$$\frac{dy}{dt} = \eta(t). \quad (3)$$

The initial condition for probability distribution $P(l, t)$

$$P(l, 0) = \delta(l - l_0)$$

is transformed into initial condition

$$P(y, 0) = \delta(y - y(l_0))$$

due to the relationships

$$P(y, t) = \left| \frac{dl}{dy} \right| P(l, t)$$

and

$$\delta(y(l) - y(l_0)) = \frac{1}{\left| \frac{dy}{dl} \right|} \delta(l - l_0).$$

Therefore we obtain from (3) the log-normal distribution

$$P(l) = \frac{1}{(4\pi\sigma^2 t)^{1/2}} l^{-1} \exp \left[-\frac{(\ln l/l_0)^2}{4\sigma^2 t} \right] \quad (4)$$

(cf [12] for another derivation of log-normal and power-law asymptotics and their application to fragmentation).

For $n > 1$, substitution

$$y = \frac{1}{(1-n)} l^{1-n} \quad (5)$$

again transforms equation (1) into (3) and we obtain the corresponding probability distribution in the form

$$P(l) = \frac{1}{(4\pi\sigma^2t)^{1/2}} l^{-n} \exp\left[-\frac{(l^{1-n} - l_0^{1-n})^2}{4\sigma^2(1-n)^2t}\right]. \quad (6)$$

It should be noted that this distribution is close to a modified Weibull distribution [13]. For

$$\frac{(l^{1-n} - l_0^{1-n})^2}{4\sigma^2(1-n)^2t} \ll 1 \quad (7)$$

we obtain from (6) the power-law distribution

$$P(l) \sim l^{-n}. \quad (8)$$

One may also expect significant deviation from the asymptotic Gaussian distribution when t is not large, i.e. when there is only a finite number of branching, which is bound to occur in real experiments.

In the numerical simulations and experiments the probability distributions of *mass* of fragments are usually calculated. For the approximately isotropic situation (in some interval of scales) we can use the relation

$$m \sim l^d \quad (9)$$

where d is the space dimension. Then we obtain from (6)

$$P(m) \sim m^{-\beta} \exp[-a(m^{(1-n)/d} - m_0^{(1-n)/d})^2] \quad (10)$$

where

$$\beta = \frac{d+n-1}{d} \quad (11)$$

and a is some constant. Thus we have the following classification scheme:

$$n = 1 : \quad P(m) \text{ is log-normal} \quad (12)$$

$$n = 2 : \quad \beta = \frac{d+1}{d} \quad (13)$$

$$n = 3 : \quad \beta = \frac{d+2}{d}. \quad (14)$$

The situation with $n = 1$ (i.e. log-normal fragment mass distribution) can be associated with fragmentation produced by several main cracks sprouting numerous daughter branches.

The situation with $n = 2$ (i.e. a power-law fragments mass distribution) can be associated with planar (in 2D space) and cylindrical (in 3D space) wavefront propagation. In this situation we obtain from (13)

$$\beta = \frac{3}{2} \quad (\text{in 2D}) \quad \text{and} \quad \beta = \frac{4}{3} \quad (\text{in 3D}). \quad (15)$$

And finally, the situation with $n = 3$ can be associated with impact fragmentation with a volume-like nucleation manifold (such as, for instance, takes place in collisions of solids). For this situation we obtain from (14)

$$\beta = 2 \quad (\text{in 2D}) \quad \text{and} \quad \beta = \frac{5}{3} \quad (\text{in 3D}). \quad (16)$$

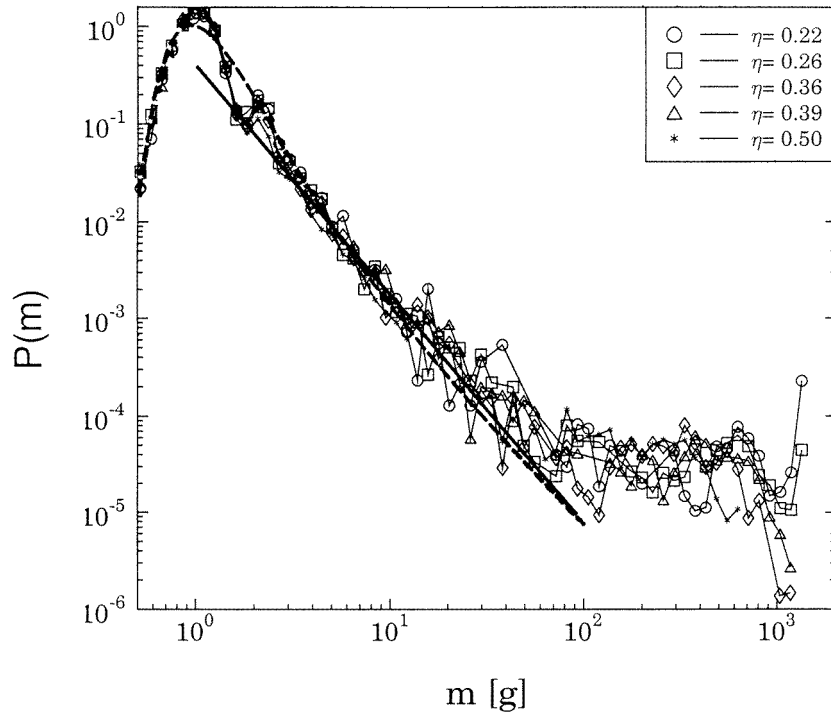


Figure 1. Mass distribution of fragments at different values of impact energy after 2D solid disc collision (data taken from numerical simulation [8]). The dashed curve indicates agreement with calculation using (10).

3. Comparison with data of experiments and numerical simulations

Observations of the log-normal distribution in experiments and numerical simulations of fracture and fragmentation processes have already been discussed in the introduction. Let us now discuss observations of the power-law distributions. In a recent numerical simulation [6] a fractured object was represented by a set of mass points connected by Hookean springs with threshold dynamics. In this numerical simulation fragmentation processes were studied for different conditions. In particular, for 2D fragmentation by impulsive load from one side of a square crystal (this situation corresponds to plane wavefront propagation) the author of [6] obtained a value of $\beta \simeq \frac{3}{2}$, and for 3D fragmentation initiated by sudden expansion of the cylindrical region at the centre of a cubic crystal he obtained a value of $\beta \simeq \frac{4}{3}$. These results are in good agreement with (15) ($n = 2$).

Let us discuss the third situation: $n = 3$. The value of $\beta = \frac{5}{3}$ (16) is very well known from numerous 3D experiments and numerical simulations (see, for instance, [3–6] and references therein), while a recent numerical simulation on 2D solid disc collision in 2D space [7, 8] gives $\beta \simeq 2$ (cf (16)).

In figure 1 we show data taken from [8] for different values of the impact energy. The dashed curve is drawn in this figure for comparison with (10) ($n = 3$ and $d = 2$). In computer simulations there are always two cutoffs for the fragment masses, a lower one due to the discretization and an upper one due to finite system size. This gives rise to the hump on the left side of the simulated curves. One can see in figure 1 that the calculation using (10) (the

dashed curve) gives a value of the probability density maximum smaller than those given by computer simulation. Small (within 10%) deviations of β from 2 observed in [7,8] for different values of the impact energy seem to be rather systematic and, therefore, we suppose that these deviations are related to some intermittency phenomenon as it takes place in turbulence. To take this phenomenon into account, equation (1) can be replaced by

$$\frac{dl}{dt} = \eta(t)l^n (l/L)^\delta \quad (17)$$

where δ is an intermittency exponent depending on the impact energy and L is a large-scale cutoff.

This approach suggests that the most relevant thing for describing the fragmentation process resulting in a power-law size distribution on fragment masses is the geometry of the elastic wavefront where the crack nucleation occurs. In the literature, however, it has been shown that symmetry of the shock wave with respect to the geometry of the object being fragmented also plays an important role (see, e.g., [4]). This is the reason why the exponent of the power law depends on the aspect ratio in the case of two-dimensional objects [4]. Extending the present model to take into account this phenomenon is an interesting problem for future investigation.

Acknowledgments

This work is supported by the Hong Kong Research Grants Council (Grant no 315/96P). The authors are grateful to J Fineberg for stimulating correspondence, and to N Schörghofer for discussions. The referee's comments and suggestions were very useful for improving the paper.

References

- [1] Sharon E and Fineberg J 1996 *Phys. Rev. B* **54** 7128
- [2] Fineberg J and Marder M 1999 *Phys. Rep.* **313** 1
- [3] Gilvarry J J and Bergstrom B H 1961 *J. Appl. Phys.* **32** 400
- [4] Oddershede L, Dimon P and Bohr J 1993 *Phys. Rev. Lett.* **71** 3107
- [5] Inaoka H, Toyasawa E and Takayasu H 1997 *Phys. Rev. Lett.* **78** 3455
- [6] Hayakawa Y 1996 *Phys. Rev. B* **53** 14 828
- [7] Kun F and Herrmann H J 1996 *Int. J. Mod. Phys. C* **7** 837
- [8] Kun F and Herrmann H J 1999 *Phys. Rev. E* **59** 2623
- [9] Mori Y, Kaneko K and Wadati M 1991 *J. Phys. Soc. Japan* **60** 1591
- [10] Marder M and Liu X 1993 *Phys. Rev. Lett.* **71** 2417
- [11] Gross S 1995 *J. Mech. Phys. Solids* **43** 1
- [12] Frisch U and Sornette D 1997 *J. Physique I* **7** 1155
- [13] Bradley C E and Price T 1992 *Appl. Math. Comput.* **50** 115